J Mater Sci: Mater Electron
DOI 10.1007/s10854-016-6116-7

Controlling recombination kinetics of hybrid poly-3-hexylthiophene (P3HT)/titanium dioxide solar cells by self-assembled monolayers

S. Loheeswaran[1,2] · M. Thanihaichelvan[1] · P. Ravirajan[1] · J. Nelson[3]

Received: 18 September 2016 / Accepted: 18 November 2016

Abstract Self-assembled monolayers (SAMs) of benzoic acid based molecules are used to modify the metal oxide–polymer interface in a hybrid poly-3-hexylthiophene (P3HT)/TiO_2 photovoltaic device structure. The effect of SAMs on current density is in accordance with expectation from the driving force for charge separation of metal oxide–polymer interface in a hybrid poly-3-hexylthiophene (P3HT)/TiO_2 photovoltaic device. However, the effect of monolayers on open circuit voltage is quite unexpected from the interfacial energetics as all the monolayers improve the open circuit voltage in spite of different sign of the interfacial dipole for different SAMs. This suggests that the monolayers have additional functions. Overall device performance is enhanced by more than a factor of two using a SAM with permanent dipole pointing towards the TiO_2 surface or pointing towards polymer when compared to a control device with no interface modifiers. This study concludes that the SAM layer has two functions that are to shift the position of the conduction band of the porous TiO_2 relative to the polymer HOMO level so as to influence interfacial charge separation and to act as a barrier layer, insulating back electron transfer from the TiO_2 to the polymer. Both effects can benefit the performance of hybrid polymer metal oxide solar cells.

✉ P. Ravirajan
p_ravirajan@jfn.ac.lk; pravirajan@gmail.com

[1] Department of Physics, Faculty of Science, University of Jaffna, Jaffna 40000, Sri Lanka

[2] Department of Physical Science, Trincomalee Campus, Eastern University, Trincomalee, Sri Lanka

[3] Department of Physics, Imperial College London, London SW7 2BW, UK

1 Introduction

Composites of conjugated polymers with nanostructured metal oxides are promising material combinations for low-cost solar energy conversion [1, 2]. However, the performance of devices based on such structures is still limited by several factors, including inefficient exciton dissociation and interfacial charge recombination. The interfacial phenomena play a central role in these types of solar cells because, charge separation and charge recombination are all interfacial processes [3, 4]. A large interfacial area is required for efficient exciton dissociation but tends to increase interfacial recombination rates [5]. One strategy to address this issue is to control the interfacial charge transfer rates by modifying the electronic properties of the interface [6–9]. An appropriate alignment of the energy levels between donor and acceptor layers is fundamental for efficient exciton dissociation and subsequent charge separation; a large energy differences between them makes the exciton dissociation possible, promotes efficient separation of the charges, and suppresses interfacial charge recombination. For this reason, tuning the interfacial properties is very important in improving the device performance.

It has been reported that by modifying the interface between the metal oxide and polymer layer by using SAM molecules, the morphology and charge selectivity of the hybrid polymer solar cell can be improved simultaneously. [10, 11] This phenomenon can be attributed to the mechanisms such as increased tunnelling probability due to reduced effective barrier, energy level realignment induced by interfacial dipole and elimination of exciton quench centres [10, 12]. Furthermore SAMs have been shown to significantly change the interfacial properties of various oxide and metallic surfaces. They can be used to improve

Published online: 30 November 2016

adhesion, compatibility, wettability and charge transfer properties at the interface to reduce back charge recombination [8]. In addition, they can also be used to control the upper layer growth mode and distribution of phases, passivate inorganic surface trap states, and shift the interfacial energy offset between donor–acceptor materials [6, 13].

Several studies of the use of SAMs to control the energetics at metal–organic interfaces in organic devices have been reported [14–17]. Such studies extended to the modification of dense TiO_2 substrates in order to control hole injection into a molecular organic semiconductor [18]. In addition, studies of the modification of the metal oxide—dye interface in dye-sensitised structures, using treatments such as Li+ , acid or base over layers, tert-butylpyridine, and ambiphilic or deprotonated dye molecules, show that charge separation yield and kinetics are sensitive to the energetic structure at this interface [19–21].

When a SAM is applied to an oxide surface, the dipole at the donor–acceptor interface modifies the interface energy offset upon attachment [22]. This observation was attributed to the presence of dipole fields, building up upon self-assembly of molecular dipoles on a surface. In addition to affecting the energy levels of the donor–acceptor pair, the molecular orbital of the SAM's molecule form electronic states at the interface, which may block or mediate forward charge transfer or reduce back charge recombination.

The self-assembled monolayer (SAM) attaches to the TiO_2 surface via the carboxylate group, the sign of the dipole moment for each SAM is determined by the electron-withdrawing or donating character of the chemical substituent in the para position. The NO_2 group in 4-Nitro Benzoic Acid (NBA; see Fig. 1a) is electron accepting, leading to a dipole moment pointing towards the TiO_2 surface and a corresponding increase in TiO_2 work function, while the methoxy group in 4-Methoxy Benzoic Acid (MBA; see Fig. 1b) is electron donating and leads to a dipole moment pointing away from the TiO_2 surface and a decrease in TiO_2 work function [6].

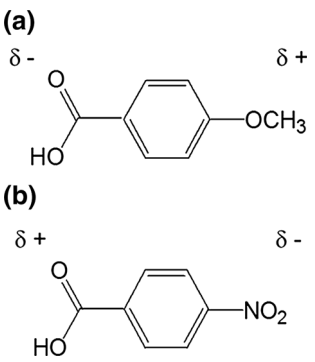

Fig. 1 Chemical structure of **a** MBA with dipole moment of −3.9 and **b** NBA with dipole moment of 3.8 (the dipole moments are derived from density function theory)

It has been reported by Ishwara et al. [23] that V_{OC} correlates very well with the dipole magnitude. Dipole pointing towards TiO_2 decrease V_{OC} as much as 0.2 V and increase in J_{SC} by a factor of two, whereas dipole pointing away from the TiO_2 only increase V_{OC} by at most 0.03–0.05 V and indicated the presence of a dipole layer changing the effective energy difference between the highest occupied molecular orbital (HOMO) of the polymer and the conduction band edge of the TiO_2 (HOMO − E_C) consequently affects the maximum attainable V_{OC}. They also indicated, although the maximum V_{OC} attainable is thermodynamically limited by this gap, the actual V_{OC} observed critically depends on the recombination kinetics of charge carriers [22].

In this work, we report the use of SAMs of molecules with permanent dipoles to control the interfacial electron transfer dynamics in polymer/porous TiO_2 structures, and hence to control the performance of the corresponding photovoltaic devices. Hole transporting polymer, namely P3HT, and two self-assembling permanent-dipole molecules, with opposite sign of two dipole namely NBA, and MBA were used in this study. The chemical names and structures are presented in Fig. 1a, b.

2 Materials and methods

The TiO_2 electrodes, consisting of an ITO coated glass substrate with a 50 nm thick dense TiO_2 layer and a ~600 nm thick mesoporous TiO_2 layer was deposited by spray pyrolysis as described in Ref [8]. Dipole modification was achieved by firstly heating the mesoporous TiO_2 films at 110 °C for 10 min to remove surface water, followed by soaking in a 1 mM solution of NBA or MBA in tetrahedrafuran (THF) for 2 h. Samples were then rinsed in THF and dried in nitrogen gas. Identical porous TiO_2 films without SAM coating were subjected to similar heat treatment and soaking in THF solution, in order to act as control structures. The work functions of the uncoated and SAM-coated porous TiO_2 electrodes were measured in nitrogen using a Besocke Delta-Phi Kelvin probe set-up with a 2 mm circular gold reference electrode. Hybrid P3HT/TiO_2 structures were prepared by first dip-coating the TiO_2 electrodes in 1 mg/ml P3HT solution in dichlorobenzene (DCB) for 18 h at 120 °C and then spin coating a 25 mg/ml P3HT solution in DCB to form a polymer layer of effective thickness 50 nm. Optical absorbance of the structures was measured using a UV–Vis spectrometer (Jenway 6800). Photoinduced charge transfer yield and recombination kinetics were measured using transient optical spectroscopy. Photovoltaic devices were

made by thermal evaporation of Au top contacts after deposition of a poly(ethylenedioxythiophene):polystyrene sulphonate (PEDOT: PSS) layer, as in Ref [24, 25]. Current–voltage measurements were taken in the dark or under simulated AM 1.5 irradiation.

3 Results and discussion

Kelvin probe measurements yielded work function values of 4.2 (±0.1) eV for uncoated porous TiO_2, 4.7 (±0.1) eV for NBA coated TiO_2 and 3.4 (± 0.1) eV for MBA coated TiO_2. These shifts are in accordance with expectation, as the work function difference due to the adsorbed monolayer is proportional to the dipole moment of the adsorbed molecule perpendicular to the surface. As the SAM attaches to the TiO_2 surface via the carboxylate group, the sign of the dipole moment for each SAM is determined by the electron withdrawing or donating character of the chemical substituent in the para position. The $–NO_2$ group in NBA is electron accepting, leading to a dipole moment pointing towards the TiO_2 surface and a corresponding increase in work function, while the methoxy group in MBA is electron donating and leads to a dipole moment pointing away from the TiO_2 surface and a decrease in work function. Our results are in agreement with previous studies [6, 26]. Concerning the interfacial energetics in a hybrid P3HT/TiO_2 structure, we expect that treatment with NBA will shift the conduction band edge of TiO_2 down relative to the HOMO of the P3HT, while MBA will shift the TiO_2 conduction band edge up, as illustrated in Fig. 2a, b.

Figure 3a shows the photoinduced transient absorbance for TiO_2/P3HT structures made with SAM-coated and uncoated mesoporous TiO_2 films. Figure 3b shows the same data normalised with their respective peaks. These data show that NBA treatment increases the charge transfer yield by about 30% compared to the control, but has a negligible effect on the normalised recombination kinetics. Although polymer uptake of MBA coated TiO_2 electrode is much higher than its corresponding control as well as NBA coated TiO_2 electrode, MBA treatment has a weak influence in charge transfer yield but strong influence on the recombination time, by an order of magnitude.

Figure 4a, b shows the current density–voltage (J–V) characteristics of ITO/TiO_2/SAM^d/P3HT/PEDOT:PSS/Au devices in the dark and under illumination. Under illumination, NBA treatment results in an increase in J_{SC} about a factor of two whilst MBA treatment has also slightly increases the J_{SC}. In NBA, the electron-withdrawing moiety is designed on the opposite side of the –COOH anchoring group to produce a molecular dipole directed toward the TiO_2 surface and raise the electron affinity of molecules, especially in the region near TiO_2, assign to increased J_{SC}.

Both SAM treatments resulted in an increase of V_{OC} and J_{SC} relative to the control. The dark current has been observed to decrease with both of the SAM treatments, which is reflected in the increased V_{OC} most probably assigned due to the suppressed interfacial charge recombination.

Figure 5 shows the UV–Vis optical absorption spectra of NBA and MBA adsorbed on a 600 nm thick nanoporous TiO_2 film and dipped into the P3HT (1 mg/ml in DCB)

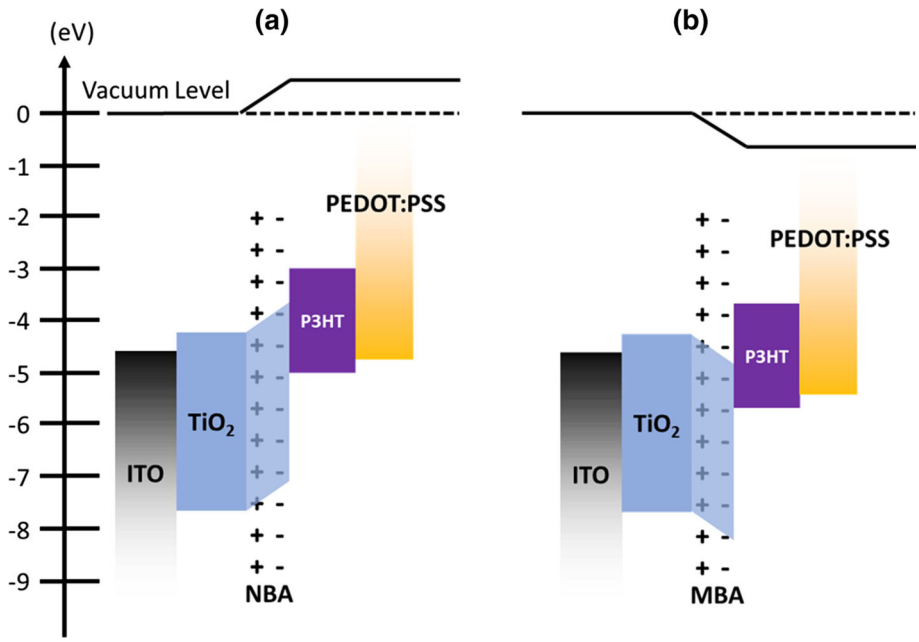

Fig. 2 **a** Energy band diagrams for ITO/TiO_2/NBA^d/$P3HT^{d,s}$/PEDOT:PSS/Au device, and **b** ITO/TiO_2/MBA^d/$P3HT^{d,s}$/PEDOT:PSS/Au device, where superscripts *d* and *s* indicate dip and spin-coated layers, respectively

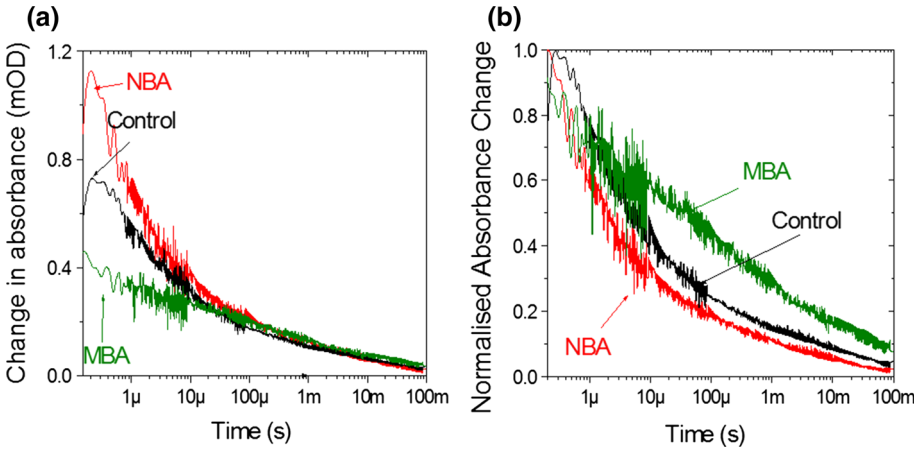

Fig. 3 **a** Transient absorption signals for TiO_2/P3HT structures made with SAM-coated and uncoated TiO_2 and **b** the normalised transient absorption signals. The transient absorption signals are assigned to the positive polaron state of the P3HT at 900 nm following laser pulse excitation at 532 nm, at an excitation density of 30 μJ/pulse/cm^2. The decay is assigned to recombination between electrons in TiO_2 and $P3HT^+$ polarons

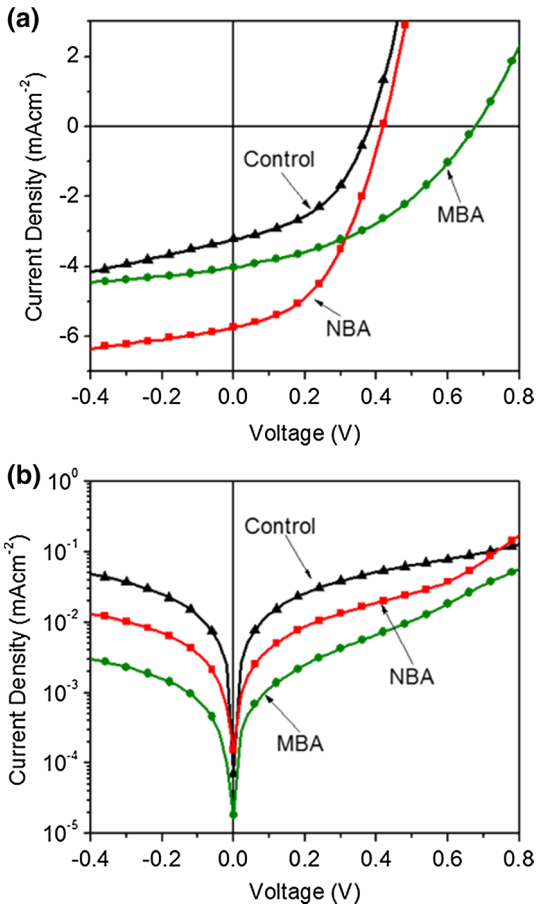

Fig. 4 **a** Current density–voltage (J–V) characteristic curve under illumination (AM 1.5, 100 mW/cm^2) and **b** semi-log version of the J–V characteristic curve in the dark

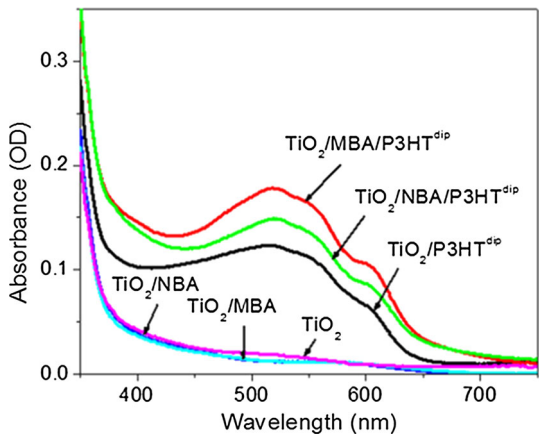

Fig. 5 UV–Vis optical absorption spectra of NBA and MBA adsorbed on a 600 nm thick nanoporous TiO_2 film and dipped into the P3HT (1 mg/ml in DCB) solutions for 18 h at 120 °C

solutions for 18 h at 120 °C. From Fig. 5, it can be shown that both of SAM attached on metal oxide surface have negligible influence on UV visible absorption spectrum but both molecules mediate better polymer uptake/adsorption on the TiO_2 film. Both NBA and MBA molecules have amphiphilic nature therefore when attached to metal surface this amphiphilic nature of the metal oxides improves interactions with polymers as described by Wang et al. [27]. In this way the dipole molecules improve the compatibility between the polymer and TiO_2 nanocrystals. Higher polymer uptake of SAM treated nanoporous electrodes in comparison with the bare film as shown in the Fig. 5 might also be contributed for the improvement in J_{SC} for the both treatments and in particular the result of unexpected improvement in J_{SC} due to MBA treatment.

As depicted in Fig. 4a and Table 1, the NBA treated device showed almost a factor of two increment in the J_{SC} and slightly improved V_{OC}. The MBA treated device on the other hand shown significant improvement in V_{OC}.

From the energy level diagram in Fig. 2 (b) we would expect that NBA treatment would increase the driving force for electron transfer from polymer to TiO_2, and decrease the energy difference (HOMO − Ec) between the HOMO level of the polymer and the conduction band edge (E_C) of the TiO_2. This increased driving force would tend to increase the charge separation yield, and hence

Table 1 Effects of the SAM treatment and its control on device merit performance

Device	J_{SC} (mA/cm^2)	V_{OC} (V)	FF	Efficiency (%)
Control device	3.1	0.37	0.40	0.47
NBA treated device	5.9	0.41	0.44	1.05
MBA treated device	4.0	0.67	0.46	1.24

photocurrent generation. The smaller E_C − HOMO separation is expected to increase the interfacial charge recombination rate and also to decrease the quasi-Fermi level separation in an illuminated structure; both factors would tend to reduce V_{OC}. On the other hand, MBA would be expected to decrease the charge separation yield but increase the E_{CB}–HOMO separation, leading to slower recombination and a larger quasi-Fermi level separation, and hence a larger V_{OC}.

The effect of NBA in increasing charge transfer yield and J_{SC} is thus in accordance with expectation from the driving force for charge separation. The absence of a significant effect of MBA treatment on J_{SC} is surprising and it may be due to increased polymer uptake as shown in Fig. 5. Nevertheless, the effect of both NBA and MBA treatments on J_{SC} are in accordance with the transient absorption spectral measurements. The effect of MBA treatment on V_{OC} is in accordance with the slower recombination and the expected effect of the quasi-Fermi level separation in the device. However, the effect of NBA to increase V_{OC} even further is quite unexpected from the interfacial energetics. The fact that both SAM layers result in an increase in V_{OC} despite the different energy level structure suggests that the SAM has an additional function. We propose that this secondary function is to act as an insulating layer, suppressing back electron transfer from the TiO_2 to the HOMO level of the polymer. A similar effect of interface layers on V_{OC} of dye or polymer sensitised metal oxide has been observed for a range of treatments, including metal oxide and sulfide overlayers [9, 20] and ambiphilic dye molecules [28].

4 Conclusion

It has been found that SAM on TiO_2 nanoparticles increases short circuit current density and open circuit voltage and hence increases the overall efficiency by a factor of two. This is attributed to the suppression of interfacial recombination and better polymer uptake by the SAM molecules. Incorporation of SAM enhances photocurrent generation and suppresses charge carrier recombination. We therefore conclude that the SAM layer has two functions: (1) shifting the position of the conduction band of the porous TiO_2 relative to the polymer HOMO level so as to influence interfacial charge separation and (2) acting as a barrier, reducing back electron transfer from the TiO_2 to the polymer.

References

1. S.H. Liao, H.J. Jhuo, P.N. Yeh, Y.S. Cheng, Y.L. Li, Y.H. Lee, S. Sharma, S.A. Chen, Sci. Rep. **4**(6813), 1–7 (2014)
2. T. Xu, Q. Qiao, Energy Environ. Sci. **4**(8), 2700–2720 (2011)
3. C.C. Chueh, C.Z. Li, A.K.Y. Jen, Energy Environ. Sci. **8**(4), 1160–1189 (2015)
4. S. Chen, J.R. Manders, S.W. Tsang, F. So, J. Mater. Chem. **22**(46), 24202–24212 (2012)
5. P. Ravirajan, A.M. Peiró, M.K. Nazeeruddin, M. Graetzel, D.D.C. Bradley, J.R. Durrant, J. Nelson, J. Phys. Chem. B **110**(15), 7635–7639 (2006)
6. J. Krüger, U. Bach, M. Grätzel, Adv. Mater. **12**(6), 447–451 (2000)
7. C. Goh, S.R. Scully, M.D. McGehee, J. Appl. Phys. **101**(11), 114503 (2007)
8. S. Loheeswaran, K. Balashangar, J. Jevirshan, P. Ravirajan, J. Nanoelectron. Optoelectron. **8**(6), 484–488 (2013)
9. M. Thanihaichelvan, K. Sockiah, K. Balashangar, P. Ravirajan, J. Mater. Sci.: Mater. Electron. **26**(6), 3558–3563 (2015)
10. S. Khodabakhsh, B. Sanderson, J. Nelson, T.S. Jones, Adv. Funct. Mater. **16**(1), 95–100 (2006)
11. J.S. Kim, J.H. Park, J.H. Lee, J. Jo, D.Y. Kim, K. Cho, Appl. Phys. Lett. **91**, 112111 (2007)
12. B. Delgertsetseg, N. Javkhlantugs, E. Enkhtur, Y. Yokokura, T. Ooba, K. Ueda, C. Ganzorig, M. Sakomura, Org. Electron. **23**, 164–170 (2015)
13. A. Khassanov, H.G. Steinrück, T. Schmaltz, A. Magerl, M. Halik, Acc. Chem. Res. **48**(7), 1901–1908 (2015)
14. S. Khodabakhsh, D. Poplavskyy, S. Heutz, J. Nelson, D.D.C. Bradley, H. Murata, Adv. Funct. Mater. **14**(12), 1205–1210 (2004)
15. D. Cahen, A. Kahn, Adv. Mater. **15**(4), 271–277 (2003)
16. A. Abrusci, S.D. Stranks, P. Docampo, H.L. Yip, A.K.Y. Jen, H.J. Snaith, Nano Lett. **13**(7), 3124–3128 (2013)
17. S.K. Hau, Y.J. Cheng, H.L. Yip, Y. Zhang, H. Ma, A.K.Y. Jen, ACS Appl. Mater. Interfaces **2**(7), 1892–1902 (2010)
18. M. Carrara, F. Nüesch, L. Zuppiroli, Synth. Met. **121**(1–3), 1633–1634 (2001)
19. G.R.R.A. Kumara, K. Tennakone, V.P.S. Perera, A. Konno, S. Kaneko, M. Okuya, J. Phys. D Appl. Phys. **34**(6), 868–873 (2001)
20. J.N. Clifford, E. Palomares, M.K. Nazeeruddin, M. Gratzel, J. Nelson, X. Li, N.J. Long, J.R. Durrant, J. Am. Chem. Soc. **126**(16), 5225–5233 (2004)
21. E. Palomares, C.N. Clifford, A. Haque, T. Lutz, J.R. Durrant, Chem. Commun. **14**, 1464–1465 (2002)
22. C. Goh, S.R. Scully, M.D. McGehee, J. Appl. Phys. Lett. **101**, 114503–114515 (2007)
23. T. Ishwara, D.D.C. Bradley, J. Nelson, P. Ravirajan, I. Vanseveren, T. Cleij, D. Vanderzande, L. Lutsen, S. Tierney, M. Heeney, I. McCulloch, Appl. Phys. Lett. **92**(5), 053308 (2008)

24. M.D. McGehee, MRS Bull. **34**(2), 95–100 (2009)
25. Y. Kim, A.M. Ballantyne, J. Nelson, D.D.C. Bradley, Org. Electron. **10**(1), 205–209 (2009)
26. M. Shalom, S. Rühle, I. Hod, S. Yahav, A. Zaban, J. Am. Chem. Soc. **131**(29), 9876–9877 (2009)
27. P. Wang, S.M. Zakeeruddin, J.E. Moser, M.K. Nazeeruddin, T. Sekiguchi, M. Gratzel, Nat. Mater. **2**, 402–407 (2003)
28. A.M. Peiro, P. Ravirajan, K. Govender, D.S. Boyle, P. O'Brien, D.D.C. Bradley, J. Nelson, J.R. Durrant, J. Mater. Chem. **16**(21), 2088–2096 (2006)